Reactive Uptake of O_3 by Multicomponent and Multiphase Mixtures Containing Oleic Acid

Daniel A. Knopf, Lori M. Anthony, and Allan K. Bertram*

Department of Chemistry, University of British Columbia, 2036 Main Mall, Vancouver, British Columbia, Canada V6T 1Z1

Received: March 10, 2005; In Final Form: April 28, 2005

The heterogeneous reaction of O_3 with lauric acid/oleic acid (LA/OA) mixtures and myristic acid/oleic acid (MA/OA) mixtures were studied as a function of composition, physical state, and microstructure at 298 K. Lauric acid and myristic acid are both alkanoic acids, whereas oleic acid is an alkenoic acid. Additionally, we investigated the uptake of O_3 by multicomponent mixtures that closely represent the composition of meat-cooking aerosols. These measurements were performed with a rotating-wall flow-tube reactor coupled to a chemical ionization mass spectrometer. The reactive uptake coefficients (γ) of O_3 on liquid LA/OA and MA/OA solutions range from 4×10^{-4} to 7.2×10^{-4}. The γ values measured for solid−liquid LA/OA and MA/OA mixtures (which consist of solid LA or solid MA in equilibrium with a liquid) range from 2×10^{-5} to 1.7×10^{-4}. These experiments show that only 7% solid by mass in the solid−liquid mixture can decrease γ by an order of magnitude compared to the liquid mixtures. The γ values for solid−liquid mixtures that closely represent the composition of meat-cooking aerosols range from 1.6×10^{-5} to 6.9×10^{-5}. We found that γ of solid−liquid mixtures depends on the microstructure of the mixtures, which in turn depends on the method of preparing the films. Furthermore, experiments employing solid−liquid mixtures show an increase in γ with increasing film age. This can be explained either by the formation of a nonequilibrium phase followed by its relaxation to the stable phase or by Ostwald's ripening, which refers to a change in the solid microstructure due to a tendency to minimize the total surface free energy of the solid. We used the obtained γ values to estimate OA lifetimes for polluted atmospheric conditions. For liquid solutions, the lifetimes were on the order of a few minutes. The lifetimes derived for solid−liquid mixtures are up to 75 min, significantly longer than for liquid solutions. Our study emphasizes the effect of the physical state and microstructure of multicomponent mixtures on the heterogeneous chemistry.

Introduction

Aerosol particles have a significant impact on global climate by interacting directly with solar and terrestrial radiation, thereby influencing the global radiation budget.[1] Furthermore, they can modify the radiative properties of clouds, the conditions required for cloud formation, and the lifetimes of clouds, by acting as cloud condensation nuclei (CCN) and ice nuclei (IN).[1−9]

Condensed-phase organic material is abundant throughout the atmosphere.[10−15] In urban areas of the U. S., for example, organic material typically accounts for 10−40% of the fine particulate mass, and in rural and remote areas of the U. S., organic material typically accounts for 30−50% of the fine particulate mass.[16] Organic aerosols, while in the atmosphere, experience reactions with gas-phase species which potentially lead to the modification of the particle composition and morphology. These reactions, which are often referred to as heterogeneous reactions, are of importance for several reasons. They may form toxic or carcinogenic compounds; thus, they may be important for health-related issues. Heterogeneous reactions may also change the hygroscopic properties[17−20] and optical properties of organic particles, and therefore, influence the ability of these particles to act as CCN[21−24] and to scatter and absorb solar radiation. Additionally, heterogeneous reactions may change the ability of organic particles to act as IN.[25] In short, these heterogeneous reactions may dictate the importance of organic particles in atmospheric chemistry, climate, and health-related issues.

* To whom correspondence should be addressed. E-mail: bertram@chem.ubc.ca.

Over the past few years, researchers have begun to focus on the heterogeneous chemistry of organic particles.[26−32] As a first step toward understanding this chemistry, researchers have investigated single-component organic particles and films as surrogates or proxies for atmospheric organic particles. Organic particles in the atmosphere, however, are most likely multicomponent and in some cases possibly multiphase mixtures.[33,34] At present, the heterogeneous chemistry of multicomponent and multiphase organic particles is basically unexplored with few exceptions.[35] Research is needed on this topic in order to obtain a complete understanding of the heterogeneous chemistry of organic particles in the atmosphere.

One specific organic heterogeneous reaction that has been extensively studied is the reaction of O_3 and pure *cis*-9-octadecenoic acid (oleic acid).[29,36−42] Experiments using coated-wall flow-tube reactors obtained reactive uptake coefficients (γ) of O_3 on pure oleic acid (OA) of around 8×10^{-4}.[29,36,39] In contrast, reactive uptake measurements employing pure OA aerosol particles derived values ranging from 7.5×10^{-4} to 9.8×10^{-3}.[35,37,38,41,42] Gas-phase and condensed-phase products for this reaction have also been investigated.[35,36,38−42]

In the atmosphere, OA is most likely found in mixtures,[33,34] and the other components of the mixtures may influence the reaction rates, reaction mechanisms, and atmospheric lifetime of OA. Field measurements together with estimated source fluxes suggest that OA has a lifetime in the atmosphere on the order of days.[33,37] In contrast, the laboratory studies on pure OA imply the lifetime is a few minutes for typical particle diameters under polluted conditions. Studies of multicomponent

10.1021/jp0512513 CCC: $30.25
Published on Web 06/07/2005

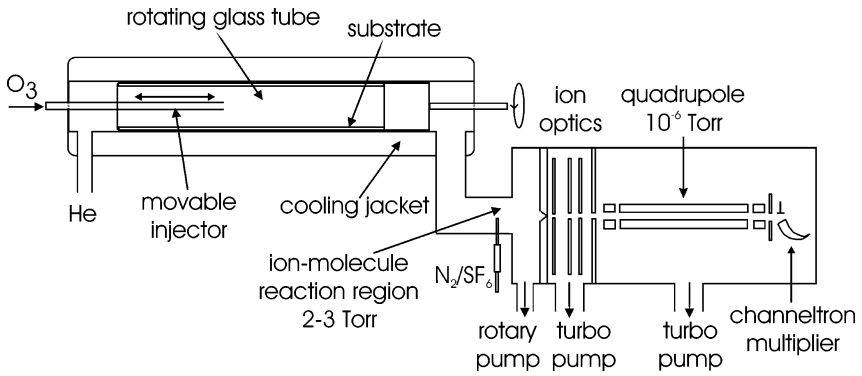

Figure 1. Sketch of the rotating-wall flow-tube reactor coupled to the CIMS.

organic aerosols are needed to better understand the lifetime and fate of OA in the atmosphere.[35]

One major source of OA-containing particles is from meat cooking.[33,34,43] These aerosol particles may comprise up to 20% of the primary fine organic carbon particle emissions in the Los Angeles area.[33] Approximately 10−20 wt % of the mass of meat-cooking particles has been identified. The composition of the identified mass is 45% *n*-alkanoic acid, 30% *n*-alkenoic acids (which is mainly OA), 3% lactones, 2% *n*-alkanes, and 3% amides.[33,34,43] A minor source of OA in the atmosphere is leaf abrasion.[44]

In the following, we present a comprehensive study of the reaction between O_3 and oleic acid/alkanoic acid mixtures. The purpose of this study is to gain a better understanding of reactions on multicomponent and multiphase organic particles, as well as to improve the understanding of the reactivity and lifetime of OA in the atmosphere. For these studies, we focused on lauric acid/oleic acid (LA/OA) and myristic acid/oleic acid (MA/OA) mixtures. LA and MA are saturated fatty acids, with 12 carbon atoms ($C_{12}H_{24}O_2$) and 14 carbon atoms ($C_{14}H_{28}O_2$), respectively. LA and MA are both significant components of aerosols from meat cooking.[33,34] In addition, the LA/OA and MA/OA systems are well-suited for the proposed studies, as both systems have a wide composition range over which the mixtures are completely liquid and also a wide composition range over which the mixtures form a solid in equilibrium with a liquid.[45] This allows us to probe systematically the effect of the phase, morphology, and OA composition on the reactivity. Additionally, we investigated the uptake on multicomponent mixtures that closely represent compositions of the identified mass of meat-cooking aerosols.[33,34] For the remainder of the document, we refer to these multicomponent mixtures as meat-cooking mixtures.

Experimental Section

Experiments were conducted in a rotating-wall flow-tube reactor coupled to a chemical ionization mass spectrometer (CIMS).[46−50] The apparatus is illustrated in Figure 1. The rotating glass tube is 1.77 cm in diameter and fits snugly inside the flow tube, which is surrounded by a cooling jacket for temperature control. O_3 enters the flow-tube reactor through a movable injector. It is important to note that in these experiments less than 3% of the OA in the films is oxidized, even for long-exposure experiments. (This was determined by comparing the total moles of OA in the films with the total moles of O_3 taken up by the films.) This is in contrast to aerosol experiments where the particles are typically completely oxidized. This should be kept in mind when comparing our experiments with aerosol experiments and also when extrapolating our results to the atmosphere.

The setup and procedure of the experiments are similar to Moise and Rudich[36] and Thornberry and Abbatt.[39] Ozone was generated by passing a flow of O_2 over an ultraviolet source (Jelight, model #600) and then stored in a 5 L bulb. In the uptake experiments, the flow of the O_2/O_3 mixture varied between 1 and 30 $cm^3\ min^{-1}$ at STP (standard temperature and pressure). The carrier gas in the experiments was He, and a flow rate of 30−100 $cm^3\ min^{-1}$ at STP was used. Under all conditions, the flow inside the reactor was laminar, based on the Reynold's number. All uptake experiments were conducted at a constant temperature of 298 K. O_3 concentrations in the flow-tube reactor of approximately 2×10^{12} to 4×10^{12} molecules cm^{-3} were used for the uptake experiments if not indicated otherwise. An O_3 concentration of 2×10^{12} molecules cm^{-3} corresponds roughly to polluted atmospheric conditions. Typical pressures in the flow tube were between 2 and 3 Torr.

O_3 was detected as O_3^- in the mass spectrometer after its chemical ionization by SF_6^-. SF_6^- was generated by passing a trace amount of SF_6 in about 1000 STP $cm^3\ min^{-1}$ N_2 through a ^{210}Po source (NRD, model Po-2031).

Shown in Figure 2 are the phase diagrams for the LA/OA and MA/OA binary systems.[45] According to the phase diagrams, the fatty acids are immiscible in the solid phase and exist as separate solid phases below the eutectic temperatures.[45] The solid circles represent the concentrations we investigated for these systems. When the LA weight percent was less than 42 wt % for the LA/OA system and the MA weight percent was less than 17 wt % for the MA/LA system, the mixtures are completely liquid at room temperature. When the concentrations of the saturated fatty acids were higher than these values, the binary solutions formed solid−liquid mixtures, where either solid LA or solid MA was in equilibrium with a liquid at room temperature, and the ratio of liquid to solid could be determined by the lever rule. These solid−liquid mixtures are also referred to as semisolid mixtures.[51−53]

Liquid films were prepared by depositing approximately 0.6 mL of the solution on the bottom surface of the inner glass tube. This tube was then rotated at 5−10 Hz and held at 298 K, resulting in a smooth liquid film on the inside surface. Two different methods were used to prepare the solid−liquid mixtures in order to investigate the effect of film preparation technique on the observed uptake coefficients. In the first method, the solid−liquid mixtures were melted and dispersed on the inside of the flow tube, which was fixed at a temperature above the complete melting temperature of the mixture. Then, while the flow tube was rotated, the temperature was decreased to room temperature at a rate of approximately 1 K/min by changing the temperature of the coolant that was circulated in the cooling jacket of the flow cell. While the temperature decreased, the film crystallized. For the remainder of the document, this will

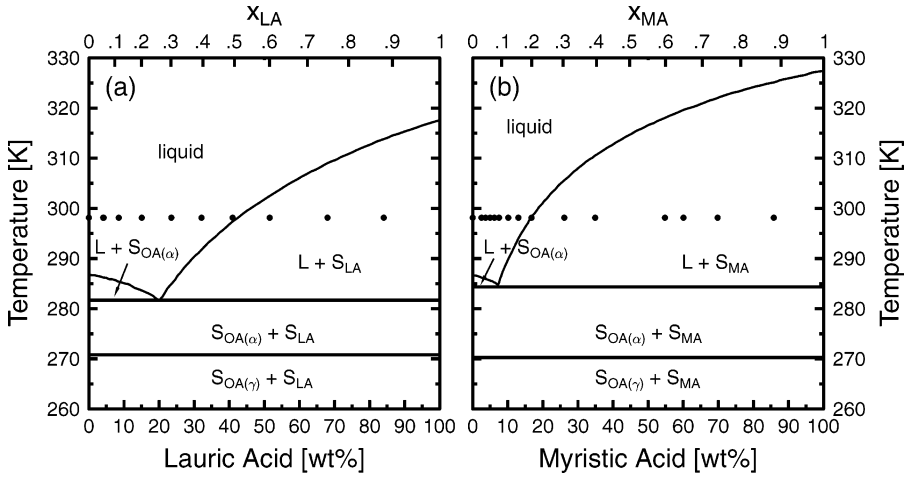

Figure 2. The phase diagrams of LA/OA and MA/OA are presented in panel (a) and panel (b), respectively, as a function of temperature and concentration.[45] S and L indicate the solid and liquid phases, respectively. x_{LA} and x_{MA} indicate the LA and MA mole fractions, respectively. $S_{OA(\alpha)}$ and $S_{OA(\gamma)}$ represent two polymorphic forms of OA.[45] The filled circles indicate the conditions of the conducted experiments.

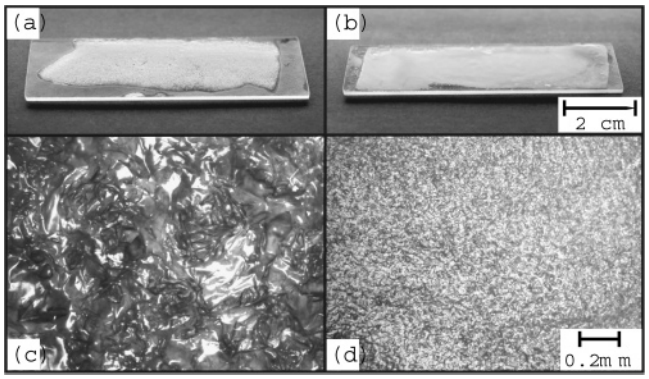

Figure 3. Panels (a) and (b) show a film composed of 51 wt % LA/OA prepared by slow and fast cooling, respectively. Panels (c) and (d) show the same films as (a) and (b) but with a higher magnification. Panels (a) and (b) were obtained with a digital camera and (c) and (d) were obtained with an optical microscope.

be referred to as slow cooling. In the second method, the solid−liquid mixture was completely melted and dispersed on the inside of a glass tube, which was preheated to above the complete melting temperature of the mixture. The glass tube was rotated to form a smooth liquid film on the inside of the glass. Then, the glass tube was rapidly immersed into liquid N_2. A similar method has been used previously to prepare solid films for uptake experiments.[54] For the remainder of the document, this will be referred to as fast cooling. Subsequently, the tube was taken out of the liquid N_2 and located inside the flow-tube reactor and held at 298 K for the uptake measurements.

Figure 3 shows images recorded with a digital camera of a 51 wt % LA/OA solid−liquid film prepared by slow (panel (a)) and fast (panel (b)) cooling. These films were prepared on microscope slides in order to record images of the films. The methods of preparing these films were the same as discussed above. For all the solid−liquid films that we prepared, the films had a very high viscosity and appeared as a solid or a wax, even when the mixture contained a significant amount of liquid based on the lever rule. The high viscosity of the solid−liquid mixtures is probably due to the microstructure of the solid in the solid−liquid system, since the rheology of solid−liquid mixtures not only depends on the solid fraction but also is highly correlated with the degree of aggregation and the interconnected network of the solid crystals in the solid−liquid mixture.[51−53,55−57] For example, previous results obtained on semisolid alloys exhibit large viscosities even at relatively low solid fractions because of the dendritic structure of the solid.[52,53,58] Shown in Figure 3 are images of the films recorded with an optical microscope. In all cases, the slow-cooled films were rougher and appeared to have larger crystals (panel (c)) than the fast-cooled films (panel (d)).

Formation of a solid−liquid mixture from a liquid solution involves nucleation and then crystal growth. The larger crystals produced by slow cooling (panel (c)) compared to fast cooling (panel (d)) can be explained by different rates of nucleation in the two methods. For slow cooling, only a few nucleation events probably occur followed by crystal growth. For rapid cooling, many nucleation events may occur, followed by crystal growth, resulting in smaller but more numerous crystals.

As mentioned above, in addition to studying the LA/OA and MA/OA systems, we studied mixtures that closely represent the composition of meat-cooking mixtures. These mixtures consisted of up to 15 different substances that correspond to the most abundant identified components of particles produced from meat-cooking processes (see below for more details). We also prepared these films using both the slow and fast cooling processes described above, and the films also appeared as solids or waxes.

We estimated the topography of the solid−liquid films using optical microscopy. First, we calibrated the *z* scale of our optical microscope using a gauge of known thickness. Then, we measured the heights of the peaks and valleys of the solid−liquid films with our microscope, while we scanned across the surfaces of the films. From this information, we estimate that the surface area of the slow- and fast-cooled films deviated from the surface area of the glass substrate by 3−8%. In all cases, we have calculated γ using the geometric surface area. Therefore, we overestimate γ by at most 8%, which is a small uncertainty compared to the overall uncertainty in the uptake measurements for solid−liquid mixtures.

Chemicals. All gases were purchased from Praxair, and solid and liquid chemicals were purchased from Aldrich. Listed below are the chemicals and the corresponding purities used in our studies: N_2 (99.999%), He (99.999%), SF_6 (99.995%), O_2 (99.993%), OA (99+%), LA (99%), MA (99.5+%), palmitic acid (99%), stearic acid (98+%), succinic acid (99.8%), glutaric acid (99%), adipic acid (99+%), palmitoleic acid (98%), tetracosane (99%), pentacosane (99%), 2-pentadecanone (98+%), 2-hexadecanone (98%), 2-octadecanone (99%), hexadecanamide (purity not verified).

Results and Discussion

Kinetics. The reactive uptake coefficients were determined from the irreversible removal of O_3 as a function of injector position. Figure 4 shows the natural logarithm of this O_3 signal as a function of reaction time (determined from the average flow velocity) for various mixtures. The data for each uptake experiment was fit to a straight line, and the observed first-order loss rate, k_{obs}, was determined from the slope.

The first-order wall loss rate, k_{wall}, was calculated from k_{obs} using the iterative numerical method of Brown,[59] which corrects for concentration gradients that form close to the flow-tube wall because of uptake at the organic surface. This results in a correction of less than 7% in all cases. The gas-phase diffusion constant of O_3 in He was taken as 394 Torr cm^2 s^{-1} at 298 K.[60,61] The reactive uptake coefficient, γ, was obtained using the equation[62,63]

$$\gamma = \frac{2rk_{wall}}{c_{O_3} + rk_{wall}} \quad (1)$$

where r is the flow-tube radius and c_{O_3} is the mean molecular velocity of O_3.

The γ values reported in this study are derived from at least three reactive uptake measurements. The reactive uptake coefficients represent the mean values of the performed uptake measurements, and the error represents two times the standard error of the mean.

Reactive Uptake Coefficients of O_3 on OA. The reactive uptake coefficients derived in this study for liquid and crystallized OA are given in Table 1. The uptake of O_3 on liquid OA at room temperature is in agreement with the previous flow-tube reactor studies by Moise and Rudich[36] and Thornberry and Abbatt.[39] Reactive uptake measurements employing pure OA aerosol particles and aerosol mass spectrometry obtained reactive uptake coefficients ranging from 7.5×10^{-4} to 9.8×10^{-3}, and in general, the γ values measured with these techniques are higher than those measured with the coated-wall flow-tube technique. A recent study by Hearn et al.[42] suggests that most of these apparent discrepancies can be explained by secondary reactions between OA and the Criegee intermediate,[64] which results from the O_3 reaction. The coated-wall technique measures the loss of O_3, whereas the aerosol measurements determine the rate of loss of OA, and therefore includes the reaction between Criegee intermediates and OA. Hearn et al.[42] estimated that approximately 36% of OA loss is due to the reaction with the Criegee intermediate, and when this value was taken into account, a reactive uptake coefficient of 8.8×10^{-4} was obtained, which is in good agreement with the flow-tube measurements. More details on the discrepancies between the aerosol studies and the flow-tube studies are given in Hearn et al.[42] Table 1 also shows the reactive uptake coefficient obtained from crystallized OA films. The γ value is approximately 1 order of magnitude lower than for the case of liquid OA. This clearly shows that the physical state of OA has a significant impact on the reactive uptake as shown previously by Moise and Rudich.[36] The small difference between the γ value derived by Moise and Rudich[36] and this study may be attributed to different surface areas or structures of the films.

Reactive Uptake Coefficients of O_3 on Liquid Binary Oleic Acid/Alkanoic Acid Mixtures. Figures 5 and 6 show the resulting reactive uptake coefficients for LA/OA and MA/OA solutions, respectively, as well as the uptake coefficient for pure OA. As the concentration of LA or MA is increased, the reactive uptake coefficient decreases as expected. However, the change

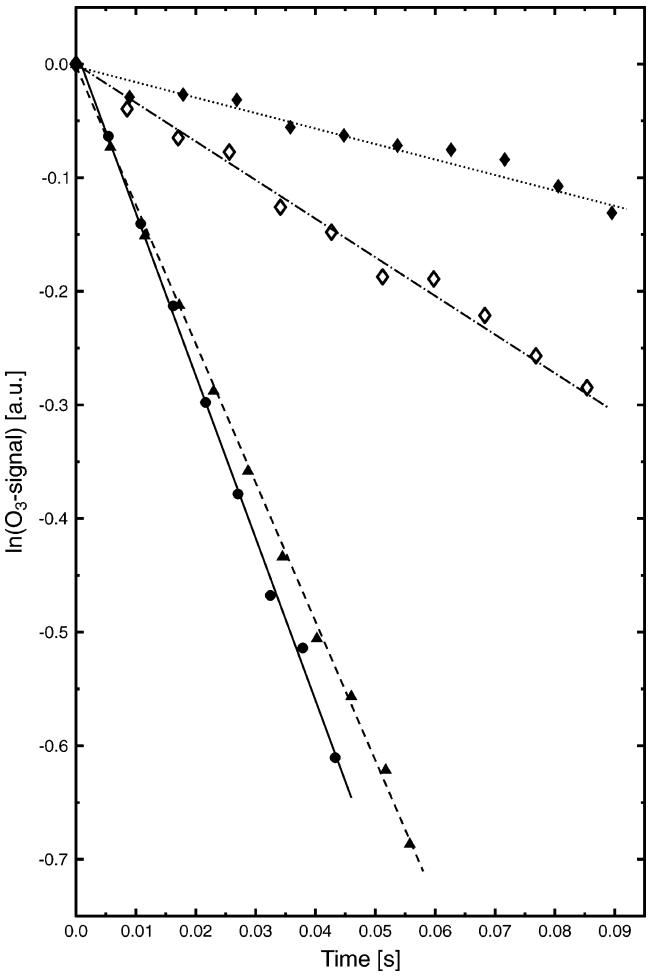

Figure 4. Natural logarithm of the observed O_3 signal as a function of reaction time. The filled circles and filled triangles correspond to uptake on pure OA and on a 32 wt % LA/OA solution, respectively. The filled and open diamonds represent the data obtained from solid−liquid 26 wt % MA/OA mixtures that have been prepared by slow and fast cooling, respectively. The lines represent the corresponding linear fits to the data.

in γ does not seem to be a continuous function. When a small amount of LA or MA is added to OA, there appears to be a step change in the uptake coefficient, after which, the uptake follows a continuous function. This step change is not large, but it appears to be bigger than the uncertainty in the measurements. (Note that each data point for LA/OA and MA/OA concentrations between 0 and 10 wt % and 0 and 4 wt %, respectively, were derived from six separate measurements in order to reduce the uncertainty in the reported values.)

Assuming that the uptake of O_3 is dominated by reaction in the bulk phase, γ can be represented by the following equation[65,66]

$$\frac{1}{\gamma} = \frac{1}{\alpha} + \frac{c_{O_3}}{4HRT\sqrt{D_{O_3}k_2[OA]}} \quad (2)$$

where α is the mass accommodation coefficient, H is the Henry's law solubility constant of O_3 in the mixture, R is the gas constant, T is the temperature, D_{O_3} is the diffusion constant of O_3 in the mixture, k_2 is the second-order rate coefficient for reaction in the condensed phase, and [OA] is the concentration of OA in the liquid. According to eq 2, a plot of $^1/_\gamma$ versus $^1/_{\sqrt{[OA]}}$ should be linear if α, H, D_{O_3}, and k_2 do not change

TABLE 1: Reactive Uptake Coefficients, γ, for O_3 on Pure Liquid and Solid OA

	this study $\times 10^{-4}$	Moise and Rudich[36] $\times 10^{-4}$	Thornberry and Abbatt[39] $\times 10^{-4}$	Morris et al.[37] $\times 10^{-4}$	Smith et al.[38] $\times 10^{-4}$	Hearn and Smith[41] $\times 10^{-4}$	Hearn et al.[42] $\times 10^{-4}$	Ziemann[35] $\times 10^{-4}$
γ (liquid)[a]	7.9 ± 0.3	8.3 ± 0.2	8 ± 1	16 ± 2[b]	58-98[b]	7.5 ± 1.2[b]	13.8 ± 0.6[b]	13 ± 2[b]
γ (solid)[c]	0.64 ± 0.05	0.52 ± 0.01						

[a] Values for γ (liquid) were obtained at temperatures between 286 and 298 K. [b] For these studies, γ values were calculated by assuming that the loss of O_3 to OA is 1:1. The recent study by Hearn et al.[42] shows that in pure OA particles the ratio is actually 1:1.36 because of the reaction between OA and the Criegee intermediate.[64] [c] Values for γ (solid) were obtained at temperatures between 278 and 285 K.

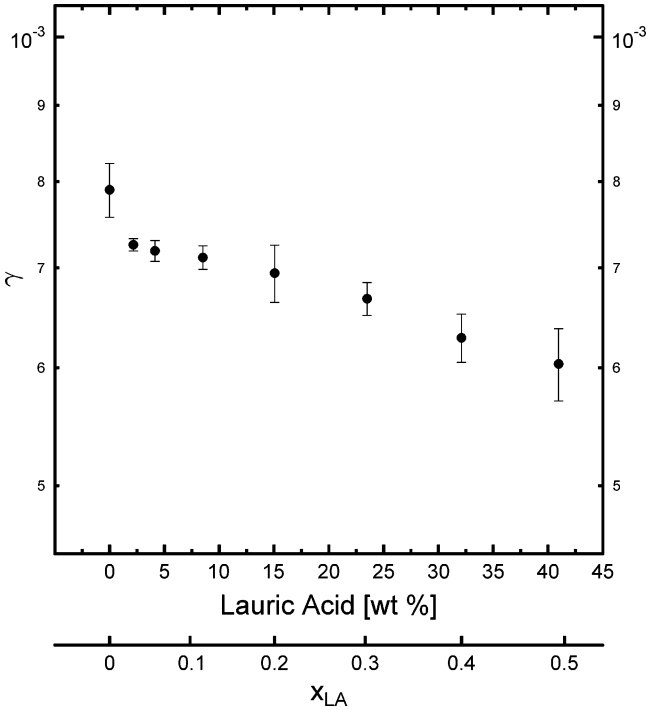

Figure 5. Experimentally derived reactive uptake coefficient, γ, as a function of LA/OA concentration conducted at 298 K. The second abscissa indicates the corresponding mole fraction.

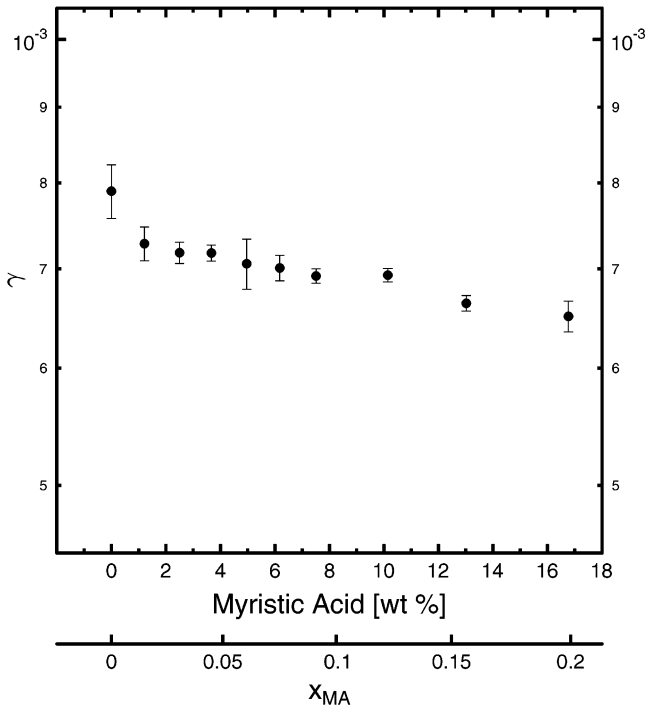

Figure 6. Experimentally derived reactive uptake coefficient, γ, as a function of MA/OA concentration conducted at 298 K. The second abscissa indicates the corresponding mole fraction.

significantly with the addition of LA or MA. Figures 7 and 8 show linear fits to all points except the data point of pure OA. Also shown are the 95% confidence intervals for the fits. In both cases, pure OA falls outside this 95% confidence interval. A possible explanation for the trend in the data is that α, H, D_{O_3}, or k_2 decrease significantly with the addition of a small amount of LA or MA.

Equation *2* assumes that the reaction occurs in the bulk and that the rate of reaction is limited by diffusion of O_3 in the liquid mixtures. Experimental data from several studies suggest that the reaction between O_3 and pure OA can be described by this model.[35−39,41] Recently, however, Hearn et al.[42] suggested (on the basis of experimental data) that the reaction occurs solely at the interface. Assuming that the uptake is governed solely by a surface reaction, γ can be represented by the following equation[67,68]

$$\frac{1}{\gamma} = \frac{1}{S} + \frac{c_{O_3}}{4k_2^S H_S RTK_S[\mathrm{OA}]} \qquad (3)$$

where S is the adsorption coefficient of O_3 on the surface, H_S is the Henry's law solubility constant of O_3 in the mixture at the surface, k_2^S is the second-order rate coefficient for reaction at the surface, and K_S is an equilibrium constant linking the surface concentration to the bulk concentration [OA]. According to eq 3, a plot of $^1/_\gamma$ versus $^1/_{[\mathrm{OA}]}$ should be linear if S, H_S, K_S, and k_2^S do not change significantly with the addition of LA or MA. Figures 9 and 10 show plots of $^1/_\gamma$ versus $^1/_{[\mathrm{OA}]}$. All data points are included in the linear least-squares analysis except the data point of pure OA. Similar to Figures 7 and 8, the data point corresponding to pure OA falls outside the 95% confidence interval for liquid LA/OA and MA/OA mixtures. We conclude that our complete data set cannot be explained by a surface reaction, assuming S, H_S, K_S, and k_2^S do not change with composition. Also, note that the quality of the linear fits shown in Figures 7 and 9 and Figures 8 and 10 are similar. Hence, we cannot determine from our data if eq 2 or eq 3 is more appropriate for the description of the reactive uptake of O_3 by liquid LA/OA and MA/OA mixtures. Further studies are needed to understand this behavior on a molecular level.

Reactive Uptake Coefficients of O_3 on Solid−Liquid Mixtures. Figures 11 and 12 show the γ values for the solid−liquid LA/OA and MA/OA mixtures, respectively. Additionally, the γ values obtained from the binary liquid solutions are plotted for comparison. The gray shading indicates the concentration over which this mixture is liquid. These figures clearly show that a small amount of solid saturated fatty acid can decrease the reactivity by an order of magnitude compared to the liquid mixtures. For example, when the slow-cooled LA/OA mixture contains only about 7% solid by mass, γ decreases by 1 order of magnitude compared to the liquid solution. The magnitude of the decrease in γ is comparable to the magnitude of the

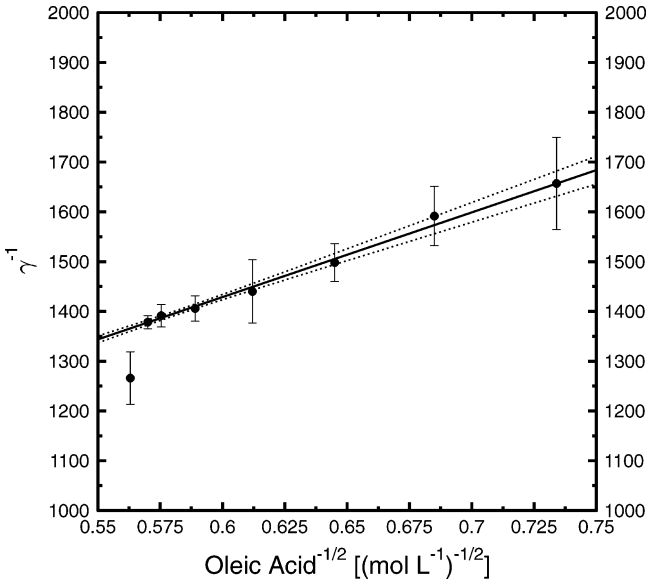

Figure 7. Plot of inverse reactive uptake coefficient vs. inverse square root of OA concentrations for LA/OA solutions. Solid line indicates a linear fit to the data points disregarding the data point of pure OA at 0.563 (mol $L^{-1})^{-1/2}$. Dotted lines represent the 95% confidence interval of the linear fit.

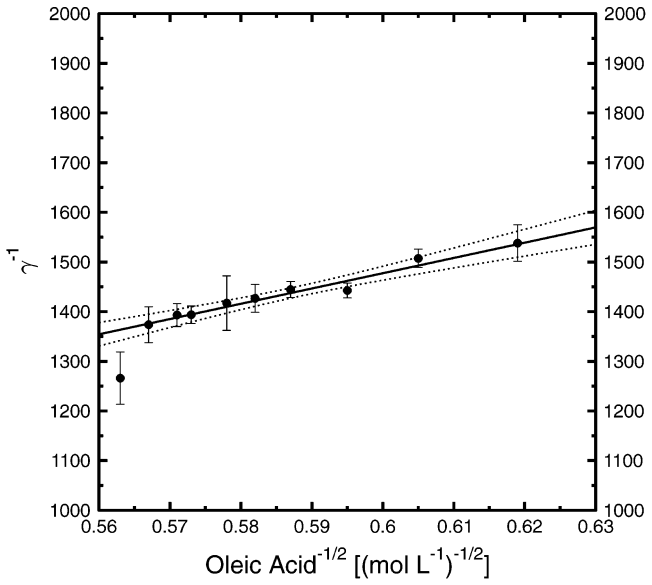

Figure 8. Plot of inverse reactive uptake coefficient vs. inverse square root of OA concentrations for MA/OA solutions. Solid line indicates a linear fit to the data points disregarding the data point of pure OA at 0.563 (mol $L^{-1})^{-1/2}$. Dotted lines represent the 95% confidence interval of the linear fit.

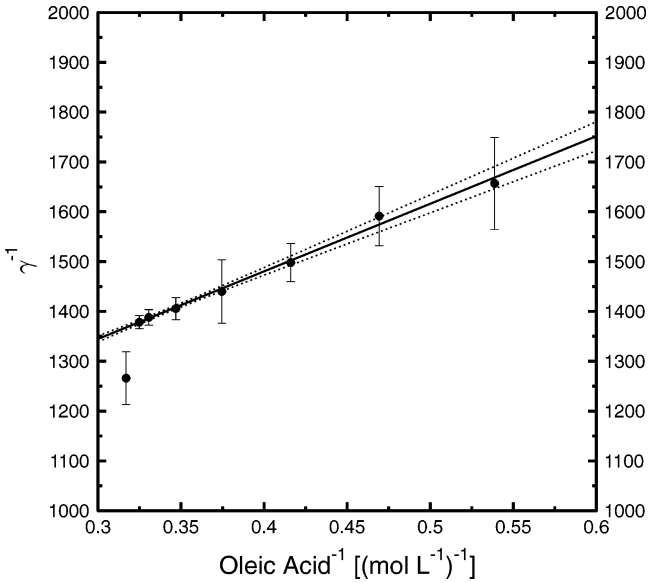

Figure 9. Plot of inverse reactive uptake coefficient vs. inverse OA concentrations for LA/OA solutions. Solid line indicates a linear fit to the data points disregarding the data point of pure OA at 0.317 (mol $L^{-1})^{-1}$. Dotted lines represent the 95% confidence interval of the linear fit.

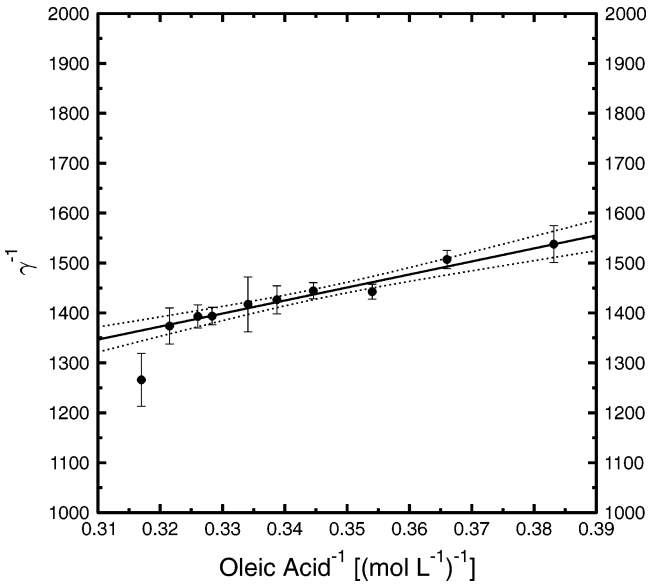

Figure 10. Plot of inverse reactive uptake coefficient vs. inverse OA concentrations for MA/OA solutions. Solid line indicates a linear fit to the data points disregarding the data point of pure OA at 0.317 (mol $L^{-1})^{-1}$. Dotted lines represent the 95% confidence interval of the linear fit.

decrease observed by Moise and Rudich[36] when going from pure liquid oleic acid to pure solid oleic acid. This behavior is most likely due to the microstructure of the solid−liquid mixtures as discussed above. The solid can form an interconnected network by dendritic growth, aggregation of crystals, or eutectic solidification, which can result in lamellar or rod microstructures.[51−53,55,56,69] An interconnected network may efficiently reduce the effective diffusion of O_3 and OA in the mixture, leading to a decrease in the uptake coefficient. Furthermore, the interconnected network may "trap" some of the OA, making it inaccessible for reaction. "Trapping" of a liquid or solvent during crystallization is a frequent problem in industrial crystallization and is associated with rapid crystallization and dendritic growth.[70] In general, the slow-cooled solid−liquid mixtures exhibit smaller reactive uptake coefficients than the fast-cooled ones. This is also most likely due to the microstructure of the solid. As shown in Figure 3, the different methods of preparing the films produce different microstructures of the solids. The microstructure produced by slow cooling appears to reduce diffusion in the mixtures or "trap" OA more efficiently than the microstructure produced by fast cooling.

Reactive uptake experiments were also performed on solid LA and solid MA films. Within the experimental uncertainty, no uptake of O_3 occurred. As mentioned above, the flow tube was rotated at 5−10 Hz in most experiments. We performed additional reactive uptake experiments on solid−liquid mixtures while the flow tube was not rotated, obtaining the same results

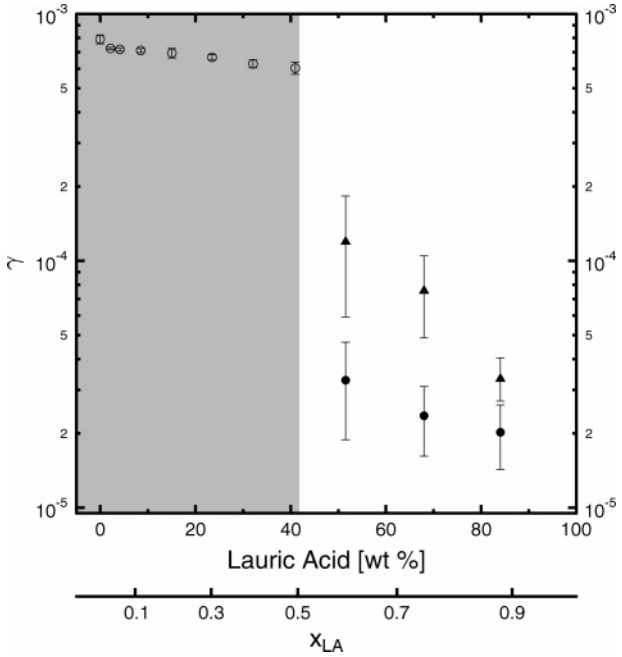

Figure 11. Experimentally derived reactive uptake coefficient, γ, as a function of LA/OA concentration. The open circles correspond to data obtained from liquid LA/OA solutions shown in Figure 5. The filled circles indicate experiments in which the mixture was cooled slowly, and the filled triangles indicate experiments in which the mixture was cooled rapidly. The second abscissa indicates the corresponding mole fraction. The gray shaded area indicates the liquid-phase concentration range.

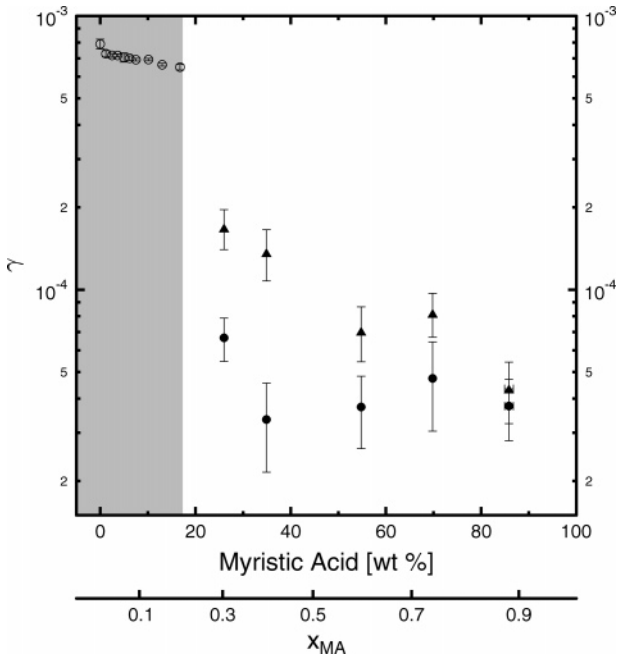

Figure 12. Experimentally derived reactive uptake coefficient, γ, as a function of MA/OA concentration. The open circles correspond to data obtained from liquid MA/OA solutions shown in Figure 6. The filled circles indicate experiments in which the mixture was cooled slowly, and the filled triangles indicate experiments in which the mixture was cooled rapidly. The second abscissa indicates the corresponding mole fraction. The gray shaded area indicates the liquid-phase concentration range.

as when the flow tube was rotated. Therefore, we conclude that the rotation has no significant effect on our uptake measurements. We have also carried out reactive uptake measurements on solid−liquid mixtures with smaller O_3 concentrations of about 7×10^{10} molecules cm^{-3}. Within our experimental uncertainty, we obtained the same results as determined with higher concentrations of ozone ($2 \times 10^{12}-4 \times 10^{12}$ molecules cm^{-3}).

Reactive Uptake Coefficients of O_3 on Solid−Liquid Mixtures That Closely Represent the Composition of Meat-Cooking Aerosols. For these studies, the experimental procedure and the data analysis are similar to that of OA and OA/alkanoic acid mixtures. As mentioned above, these mixtures are composed of up to 15 different substances that correspond to the most abundant identified components of particles produced from meat cooking.[33] The phase behavior for these multicomponent systems is not well-understood. On the basis of the enthalpies of fusion of the different components and the van't Hoff equation,[70] we speculate that the films are solid−liquid mixtures and the mixtures contain solid palmitic acid and solid stearic acid, whereas OA remains in the liquid state. This assumes that the mixtures behave as ideal solutions and that no mixed phases precipitate, and OA is not soluble in any solids that precipitate in the mixtures. Further work is needed to verify these assumptions. As determined by optical microscopy, the films appear as a solid or a wax similar to the LA/OA and MA/OA films.

Table 2 gives the experimentally obtained γ values from various mixtures (see notes[71−73] for the specific compositions). The obtained reactive uptake coefficients from these solid−liquid meat-cooking mixtures range from 1.6×10^{-5} to 6.9×10^{-5}. Mix 3[73] consists of 15 different substances and, therefore, may represent the most realistic organic mixture found in aerosol particles with respect to the identified mass.

Reactive Uptake Coefficients as a Function of Film Age. During the course of our experiments, we also discovered that the reactive uptake on semisolid mixtures increased after the films were first generated and eventually reached a maximum in γ after approximately 10 h. Shown in Figure 13 (solid triangles) are results from measurements of γ on a fast-cooled 35 wt % MA/OA solution as a function of film age. In this experiment, the film was prepared and then an uptake measurement was performed approximately every 1 h. Between measurements, the films were not exposed to ozone, but rather, they were only exposed to He gas. A similar trend in γ was observed for slow-cooled binary mixtures as well as for slow- and fast-cooled meat-cooking mixtures. We have also performed experiments where the films were exposed to O_3 continuously, and similar results were obtained. We conclude from this that the change of γ did not depend on O_3 exposure, but rather on the age of the film from which it was first prepared. For comparison, we have also included in Figure 13 the change in γ on OA as a function of the liquid film age. (In this experiment, the film was continuously exposed to O_3.) As expected, the reactive uptake on liquids does not change with film age. The increase in uptake with age was only observed for semisolid mixtures. Also, note that in our long-term experiments less than 3 % of the OA was consumed, in contrast to most aerosol experiments where the particle is completely oxidized.

The increase in the uptake coefficient with time for the solid−liquid mixtures can be explained either by Ostwald's ripening of the crystal microstructure[57,74−77] or by the formation of a nonequilibrium phase that relaxes to the stable phase.[45] The first process, Ostwald's ripening, is also referred to as particle coarsening and can be an important aging process for a solid that remains in equilibrium with the liquid.[77] This process refers to the change in the solid microstructure, driven by the tendency

TABLE 2: Obtained Reactive Uptake Coefficients and the Corresponding OA Lifetimes Given for Different Fast- and Slow-Cooled Solid−Liquid Mixtures Which Closely Represent Meat-Cooking Aerosols[a]

	mix 1[71]	mix 2[72]	mix 3[73]
n-alkenoic acids/wt%	40.0%	38.1%	37.0%
n-alkanoic acids/wt%	60.0%	49.8%	50.4%
dicarboxylic acids/wt%		2.8%	2.4%
n-alkanes/wt%		8.0%	2.6%
n-alkanones/wt%			6.0%
amides/wt%		1.3%	1.6%
γ (fast cooling)	$(6.9 \pm 1.2) \times 10^{-5}$		$(3.3 \pm 0.5) \times 10^{-5}$
γ (slow cooling)	$(4.3 \pm 0.7) \times 10^{-5}$	$(5.2 \pm 1.1) \times 10^{-5}$	$(1.6 \pm 0.3) \times 10^{-5}$
τ (fast cooling)/min	21.2		36.1
τ (slow cooling)/min	38.3	28.6	74.5

[a] The lifetime is derived for 100 ppb O_3 and particle diameters of 0.2 μm.

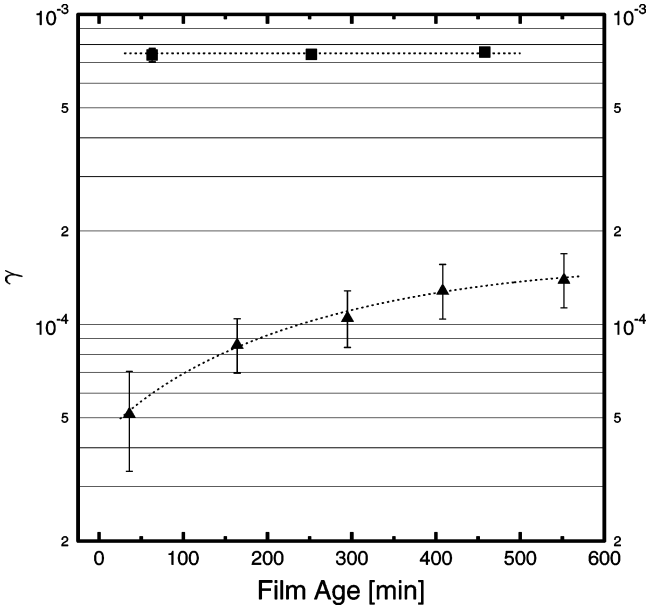

Figure 13. The O_3 uptake coefficients as a function of film age are presented for a fast-cooled 35 wt % MA/OA solution (triangles) and liquid OA (squares). The dotted lines are plotted to guide the eye and have no physical meaning.

to minimize the total surface free energy of the solid in equilibrium with a liquid.[74−77] For example, after the solidification of a dendritic structure, the solid microstructure becomes gradually coarser as a result of the remelting of dendrite arms of smaller radius.[53,77] As mentioned above, crystallization can lead to an interconnected network of solid crystals in the solid−liquid mixture by several processes including dendritic growth, aggregation, and eutectic solidification.[51−53,55−57,69,70] In general, the ripening process may decrease the connections in the solid network, which would lead to an increase of the diffusion of O_3 and OA in the solid−liquid mixture and would result in a faster uptake coefficient. The second process, the formation of a nonequilibrium phase followed by its relaxation to the stable phase, is based on the experimental findings of Inoue et al.[45] These authors suggest that when a binary LA/OA or MA/OA solution crystallizes it first forms a nonequilibrium solid in which OA is partially soluble. Following crystallization, the solid phase undergoes phase separation or so-called demixing as it relaxes toward its equilibrium state where OA is not miscible in LA or MA. This process would make more OA accessible for reaction; hence, it should lead to an increase in γ with time.

Atmospheric Implications

General Atmospheric Implications. We have shown that the uptake of O_3 on solid−liquid mixtures can be significantly smaller than the uptake on the liquid mixtures even when the solid−liquid mixture contains only a small amount of solid. We have also shown that the uptake depends strongly on the method of generating the solid−liquid mixtures. Additionally, the heterogeneous uptake coefficient increases with the age of the semisolid mixture (when the amount of the film that is oxidized is small). These findings may be important for meat-cooking aerosols and also may be important for other aerosols in the atmosphere. For example, at low relative humidities, inorganics, such as $(NH_4)_2SO_4$, may crystallize in aqueous inorganic−organic solution droplets to form solid−liquid particles.[78−80] The resulting particles may consist of an interconnected network of solid crystals in equilibrium with a liquid. This microstructure will likely influence the reactivity of these particles similar to the organic mixtures discussed above. The microstructure clearly plays an important role for the reactivity of the particles.

As mentioned above, we have shown that the uptake coefficient increases with the age of the semisolid mixture when the amount of the film that is oxidized is small. On the basis of our measurements, γ increases by approximately a factor of 2 after 10 h for semisolid films. The γ values reported in Figures 11 and 12 and Table 2, which were obtained from films less than 1.5 h in age, can be used to estimate the uptake of ozone on unoxidized particles less than approximately 2 h in age. For particles that are greater than approximately 2 h in age, the increase in γ due to Ostwald's ripening should be considered.

Atmospheric Lifetime Estimates of Oleic Acid. Reactive uptake coefficients for O_3 on OA suggest an atmospheric lifetime of OA on the order of seconds to minutes assuming O_3 concentrations of about 100 ppb[81,82] and submicron particles.[83] However, field measurements together with source fluxes suggest lifetimes on the order of days.[33,37] Morris et al.[37] and Worsnop et al.[68] speculated that the long lifetime of OA in the atmosphere is because particles in the atmosphere that contain OA are likely highly viscous and semisolid. Here, we estimate the atmospheric lifetime (which is the time it takes for the concentration of OA to decrease to $^1/_e$ of its initial value) using the γ values we derived for binary and meat-cooking mixtures. In all cases, we applied γ values which have been obtained from films less than 1.5 h in age. The increase in γ with film age as shown above has not been taken into account for these lifetime estimates. As mentioned, γ increases by approximately a factor of 2 after 10 h for solid−liquid films. The lifetimes we calculated from our measurements (see below) are at most approximately 2 h. Hence, it is more appropriate to use γ values determined from films less than 2 h in age rather than uptake coefficients determined from films 10 h in age for these calculations.

To calculate the lifetime, τ, of OA, we first determine $H\sqrt{D_{O_3}k_2}$ from our uptake measurements using eq 2 (assuming that $\alpha \gg \gamma$). Then, we use $H\sqrt{D_{O_3}k_2}$ in the following equation

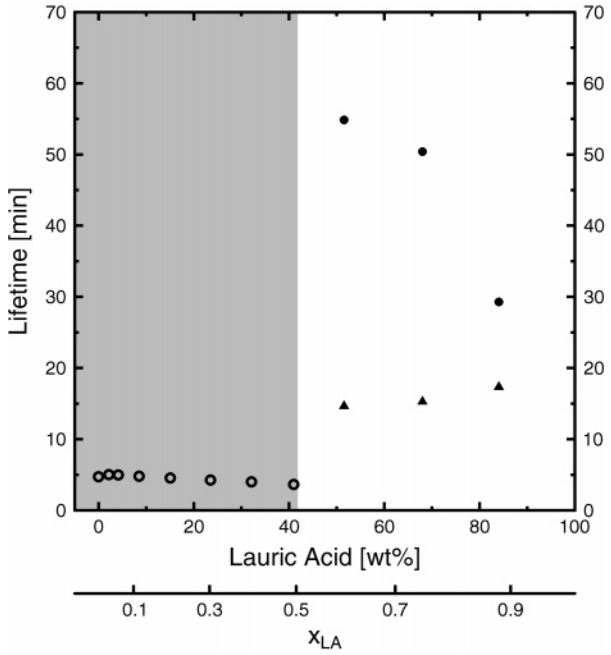

Figure 14. OA lifetimes obtained at 298 K under typical polluted environments (100 ppb O_3) for LA/OA particles, 0.2 μm in diameter. The open circles correspond to particles in the liquid state. The solid triangles and solid circles indicate particles in the solid−liquid state which have been cooled rapidly and slowly, respectively. The second abscissa indicates the corresponding mole fraction. The gray shaded area indicates the liquid-phase concentration range.

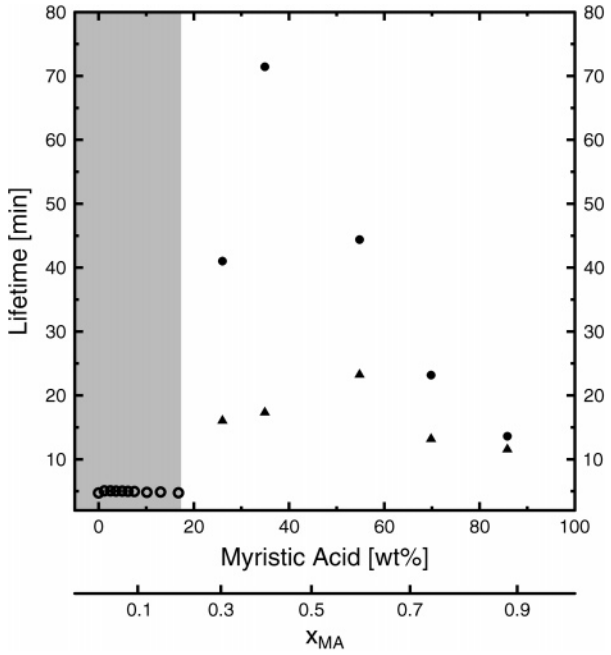

Figure 15. OA lifetimes obtained at 298 K under typical polluted environments (100 ppb O_3) for MA/OA particles, 0.2 μm in diameter. The open circles correspond to particles in the liquid state. The solid triangles and solid circles indicate particles in the solid−liquid state which have been cooled rapidly and slowly, respectively. The second abscissa indicates the corresponding mole fraction. The gray shaded area indicates the liquid-phase concentration range.

to predict the lifetime of OA in submicron particles[29,37,38]

$$\sqrt{[\mathrm{OA}]} = \sqrt{[\mathrm{OA}]_0} - \frac{3P_{\mathrm{O_3}}H\sqrt{D_{\mathrm{O_3}}k_2}}{2r}t \qquad (4)$$

where P_{O_3} is the O_3 partial pressure, t is the time the particle was exposed to O_3, r is the radius of the particle, and $[OA]_0$ is the initial OA concentration. Note that eqs 2 and 4 assume that diffusion of OA in the mixture is fast. This is most likely valid for the liquid films but may not be appropriate for solid−liquid mixtures. Nevertheless, we use these equations to estimate τ for solid−liquid mixtures in the absence of a model to describe the uptake in these mixtures. Also, note that this calculation assumes a 1:1 loss of O_3 to OA. The recent study by Hearn et al.[42] shows that in pure OA particles the ratio is actually 1:1.36 because of the reaction between OA and the Criegee intermediate.[64] However, the ratio is expected to be closer to 1:1 in LA/OA and MA/OA mixtures because of the lower concentration of OA in these solutions. From eqs 2 and 4, it follows that our assumption of 1:1 will lead at most to an overestimation of the lifetime by 36%.

Figures 14 and 15 show the derived lifetimes of aerosol particles 0.2 μm in diameter exposed to 100 ppb O_3 consisting of different LA/OA and MA/OA compositions. The lifetime τ of a pure OA particle is also plotted. The τ values range between 3.5 and 5 min for the liquid OA/alkanoic acid solutions. This shows that the lifetime of OA is not significantly modified by the addition of a second component as long as the solution remains liquid. For the solid−liquid LA/OA and MA/OA mixtures, the lifetime can change by more than an order of magnitude because of the microstructure of the solid−liquid mixtures. Lifetimes of up to 71 min are predicted for these binary solid−liquid particles.

Table 2 shows derived lifetimes which correspond to more complex meat-cooking mixtures. Lifetimes of up to 75 min are derived for mixtures containing up to 15 substances. The influence of the different temperature history on the lifetime is clearly shown. The lifetime of OA in these mixtures increased by up to a factor of 18 compared to mixtures composed of liquid OA/alkanoic solutions. Recently, Ziemann[35] also showed that lifetimes of OA in a solid−liquid mixture can be significantly longer than for pure OA.

The lifetimes above were determined with eqs 2 and 4, which assume that the reaction occurs in the bulk and that the reaction rate is limited by diffusion of O_3 in the mixtures. We have also calculated the lifetimes assuming that the reaction occurs at the surface of the particles, using eq 3 shown above and eq 16 from Worsnop et al.[68] In this case, all the calculated lifetimes were approximately 25% longer than the lifetimes calculated with the assumption that the reaction occurs in the bulk and is limited by diffusion of O_3 in the mixtures.

Our study shows how the physical state and morphology of the organic mixture can influence the reactivity and, as a consequence, alter the lifetime of OA. However, the lifetimes determined in our studies for OA may be lower limits to the lifetime of OA in the atmosphere for the following reasons: First, we have only studied uptake on the identified composition of meat-cooking aerosols, which comprise 10−20% of the total aerosol mass.[33,34] The remaining 80−90% of the mass may decrease the uptake coefficient and increase the lifetime of OA. Second, Ziemann[35] recently showed that the reactivity of solid−liquid aerosol particles consisting of palmitic acid/oleic acid and margaric acid/oleic acid decrease more than expected after approximately 50% of the OA was oxidized. In other words, two kinetic regimes were observed. As mentioned previously, less than 3% of the OA was oxidized in our experiments. If the reaction in the meat-cooking mixtures does slow down more than expected after a large fraction of the OA is oxidized, then our analysis will underestimate the lifetime of OA in the atmosphere.

Conclusions and Summary

The obtained reactive uptake coefficients for the binary liquid LA/OA and MA/OA solutions range between 4×10^{-4} and 7.2×10^{-4}. This entire data set cannot be explained by assuming that the reaction occurs exclusively in the bulk and that α, H, D_{O_3}, and k_2 do not change with composition. Furthermore, the complete data set cannot be explained by assuming that the reaction occurs at the surface and that S, H_S, K_S, and k_2^S do not change with composition.

The uptake coefficients derived from binary solid−liquid mixtures range between 2×10^{-5} and 1.7×10^{-4}, which is approximately 1 order of magnitude lower as compared to the liquid solutions. The obtained reactive uptake coefficients for mulicomponent mixtures that closely represent compositions of meat-cooking aerosols range from 1.6×10^{-5} to 6.9×10^{-5}.

We have shown that the reactive uptake coefficient is strongly dependent on the method of preparing the solid−liquid mixtures. This is most likely because the different preparation methods lead to different microstructures of the solid in the mixtures. This needs to be considered when modeling the lifetime and chemical processing of atmospheric particles. Also, this should be kept in mind when comparing laboratory results that use different preparation methods of films and particles. In some cases, a direct comparison between laboratory results may not be possible.

We observed an unexpected increase in the reactivity with time for solid−liquid OA-containing mixtures. This has been attributed to Ostwald's ripening or the relaxation of a nonequilibrium phase to the stable phase. This also needs to be considered when comparing laboratory results and when extrapolating to the atmosphere.

The OA lifetimes obtained for semisolid OA mixtures are up to a factor of 18 higher than for liquid mixtures. Lifetimes up to 75 min were obtained for these mixtures.

Acknowledgment. We thank P. Ziemann, S. T. Martin, D. Worsnop, G. D. Smith, and Y. Rudich for helpful discussions related to this manuscript and T. Inoue for helpful discussions on phase transitions and morphology of oleic acid/alkanoic acid mixtures. This work was funded by the Natural Science and Engineering Research Council of Canada, NSERC, the Canadian Foundation for Climate and Atmospheric Sciences, CFCAS, and the Canada Foundation for Innovation, CFI.

References and Notes

(1) *Climate Change 2001: The Scientific Basis. Contribution of Working Group I to the Third Assessment Report of the Intergovernmental Panel on Climate Change*; Cambridge University Press: Cambridge, United Kingdom, 2001.
(2) Twomey, S. *Atmos. Environ.* **1974**, *8*, 1251−1256.
(3) Twomey, S. *Atmos. Environ. A* **1991**, *25*, 2435−2442.
(4) Albrecht, B. *Science* **1989**, *245*, 1227−1230.
(5) Pincus, R.; Baker, M. *Nature (London)* **1994**, *372*, 250−252.
(6) Baker, M. B. *Science* **1997**, *276*, 1072−1078.
(7) Rosenfeld, D. *Science* **2000**, *287*, 1793−1796.
(8) Ramanathan, V.; Crutzen, P. J.; Kiehl, J. T.; Rosenfeld, D. *Science* **2001**, *294*, 2119−2124.
(9) Pruppacher, H. R.; Klett, J. D. *Microphysics of Clouds and Precipitation*; Kluwer Academic Publishers: Dordrecht, The Netherlands, 1997.
(10) Simoneit, B. R. T.; Cardoso, J. N.; Robinson, N. *Chemosphere* **1991**, *23*, 447−465.
(11) Simoneit, B. R. T.; Sheng, G. Y.; Chen, X. J.; Fu, J. M.; Zhang, J.; Xu, Y. P. *Atmos. Environ. A* **1991**, *25*, 2111−2129.
(12) Middlebrook, A. M.; Murphy, D. M.; Thomson, D. S. *J. Geophys. Res.* **1998**, *103*, 16475−16483.
(13) Murphy, D. M.; Thomson, D. S.; Mahoney, T. M. J. *Science* **1998**, *282*, 1664−1669.
(14) Simoneit, B. R. T.; Kobayashi, A.; Kawamura, K.; Mochida, M. *Geochim. Cosmochim. Acta* **2003**, *67*, A437−A437.
(15) Tervahattu, H.; Juhanoja, J.; Vaida, V.; Tuck, A. F.; Niemi, J. V.; Kupiainen, K.; Kulmala, M.; Vehkamäki, H. *J. Geophys. Res.* **2005**, *110*, D06207.
(16) *Air Quality Criteria for Particulate Matter*; EPA/600P-95/001; United States Environmental Protection Agency: Washington, DC, 1996.
(17) Saxena, P.; Hildemann, L. M.; McMurry, P. H.; Seinfeld, J. H. *J. Geophys. Res.* **1995**, *100*, 18755−18770.
(18) Cruz, C. N.; Pandis, S. N. *Environ. Sci. Technol.* **2000**, *34*, 4313−4319.
(19) Dick, W. D.; Saxena, P.; McMurry, P. H. *J. Geophys. Res.* **2000**, *105*, 1471−1479.
(20) Ming, Y.; Russell, L. M. *AIChE J.* **2002**, *48*, 1331−1348.
(21) Novakov, T.; Penner, J. E. *Nature (London)* **1993**, *365*, 823−826.
(22) Facchini, M. C.; Mircea, M.; Fuzzi, S.; Charlson, R. J. *Nature (London)* **1999**, *401*, 257−259.
(23) Broekhuizen, K.; Kumar, P. P.; Abbatt, J. P. D. *Geophys. Res. Lett.* **2004**, *31*, L01107.
(24) Asad, A.; Mmereki, B. T.; Donaldson, D. J. *Atmos. Chem. Phys.* **2004**, *4*, 2083−2089.
(25) Gorbunov, B.; Baklanov, A.; Kakutkina, N.; Windsor, H. L.; Toumi, R. *J. Aerosol Sci.* **2001**, *32*, 199−215.
(26) Ellison, G. B.; Tuck, A. F.; Vaida, V. *J. Geophys. Res.−Atmos.* **1999**, *104*, 11633−11641.
(27) Wadia, Y.; Tobias, D. J.; Stafford, R.; Finlayson-Pitts, B. J. *Langmuir* **2000**, *16*, 9321−9330.
(28) Moise, T.; Talukdar, R. K.; Frost, G. J.; Fox, R. W.; Rudich, Y. *J. Geophys. Res.−Atmos.* **2002**, *107*, 223−242.
(29) Rudich, Y. *Chem. Rev.* **2003**, *103*, 5097−5124.
(30) Finlayson-Pitts, B. J.; Wingen, L. M.; Sumner, A. L.; Syomin, D.; Ramazan, K. A. *Phys. Chem. Chem. Phys.* **2003**, *5*, 223−242.
(31) Eliason, T. L.; Gilman, J. B.; Vaida, V. *Atmos. Environ.* **2004**, *38*, 1367−1378.
(32) Dubowski, Y.; Vieceli, J.; Tobias, D. J.; Gomez, A.; Lin, A.; Nizkorodov, A. S.; McIntire, T. M.; Finlayson-Pitts, B. J. *J. Phys. Chem. A* **2004**, *108*, 10473−10485.
(33) Rogge, W. F.; Hildemann, L. M.; Mazurek, M. A.; Cass, G. R.; Simoneit, B. R. T. *Environ. Sci. Technol.* **1991**, *25*, 1112−1125.
(34) Schauer, J. J.; Kleeman, M. J.; Cass, G. R.; Simoneit, B. R. T. *Environ. Sci. Technol.* **1999**, *33*, 1566−1577.
(35) Ziemann, P. *Faraday Discuss.* **2005**, in press.
(36) Moise, T.; Rudich, Y. *J. Phys. Chem. A* **2002**, *106*, 6469−6476.
(37) Morris, J. W.; Davidovits, P.; Jayne, J. T.; Jimenez, J. L.; Shi, Q.; Kolb, C. E.; Worsnop, D. R.; Barney, W. S.; Cass, G. *Geophys. Res. Lett.* **2002**, *29*, 9582−9587.
(38) Smith, G. D.; Woods, E.; DeForest, C. L.; Baer, T.; Miller, R. E. *J. Phys. Chem. A* **2002**, *106*, 8085−8095.
(39) Thornberry, T.; Abbatt, J. P. D. *Phys. Chem. Chem. Phys.* **2004**, *6*, 84−93.
(40) Katrib, Y.; Martin, S. T.; Hung, H. M.; Rudich, Y.; Zhang, H. Z.; Slowik, J. G.; Davidovits, P.; Jayne, J. T.; Worsnop, D. R. *J. Phys. Chem. A* **2004**, *108*, 6686−6695.
(41) Hearn, J. D.; Smith, G. D. *J. Phys. Chem. A* **2004**, *108*, 10019−10029.
(42) Hearn, J. D.; Lovett, A. J.; Smith, G. D. *Phys. Chem. Chem. Phys.* **2005**, *7*, 501−511.
(43) Limbeck, A.; Puxbaum, H. *Atmos. Environ.* **1999**, *33*, 1847−1852.
(44) Rogge, W. F.; Hildemann, L. M.; Mazurek, M. A.; Cass, G. R.; Simoneit, B. R. T. *Environ. Sci. Technol.* **1993**, *27*, 2700−2711.
(45) Inoue, T.; Hisatsugu, Y.; Ishikawa, R.; Suzuki, M. *Chem. Phys. Lipids* **2004**, *127*, 161−173.
(46) Lovejoy, E. R.; Huey, L. G.; Hanson, D. R. *J. Geophys. Res.* **1995**, *100*, 18775−18780.
(47) Huey, L. G.; Hanson, D. R.; Howard, C. J. *J. Phys. Chem.* **1995**, *99*, 5001−5008.
(48) Hanson, D. R.; Lovejoy, E. R. *J. Phys. Chem.* **1996**, *100*, 6397−6405.
(49) Longfellow, C. A.; Imamura, T.; Ravishankara, A. R.; Hanson, D. R. *J. Phys. Chem. A* **1998**, *102*, 3323−3332.
(50) de Gouw, J. A.; Lovejoy, E. R. *Geophys. Res. Lett.* **1998**, *25*, 931−934.
(51) Koke, J.; Modigell, M. *J. Non-Newtonian Fluid Mech.* **2003**, *112*, 141−160.
(52) Barbe, J. C.; Perez, M.; Papoular, M. *J. Phys.: Condens. Matter* **2000**, *12*, 2567−2577.
(53) Flemings, M. C. *J. Phys.: Condens. Matter* **1991**, *22*, 269−293.
(54) Bertram, A. K.; Ivanov, A. V.; Hunter, M.; Molina, L. T.; Molina, M. J. *J. Phys. Chem. A* **2001**, *105*, 9415−9421.
(55) Kurz, W.; Giovanola, B.; Trivedi, R. *J. Phys.: Condens. Matter* **1986**, *34*, 823−830.
(56) Barthelmes, G.; Pratsinis, S. E.; Buggisch, H. *Chem. Eng. Sci.* **2003**, *58*, 2893−2902.

(57) Chou, C.-M.; Hong, P.-D. *Macromolecules* **2004**, *37*, 5596−5606.
(58) Wu, S. S.; Wu, X. P.; Xiao, Z. H. *Acta Mater.* **2004**, *52*, 3519−3524.
(59) Brown, R. L. *J. Res. Natl. Bur. Stand. (U.S.)* **1978**, *83*, 1−8.
(60) Fuller, E. N.; D., S.; Giddings, J. C. *Ind. Eng. Chem.* **1966**, *58*, 19−27.
(61) Moise, T.; Rudich, Y. *J. Geophys. Res.* **2000**, *105*, 14667−14676.
(62) Davison, B. *Proc. Phys. Soc. A* **1951**, *64*, 881−902.
(63) Motz, H.; Wise, H. *J. Chem. Phys.* **1960**, *32*, 1893−1994.
(64) Criegee, R. *Angew. Chem., Int. Ed. Engl.* **1975**, *14*, 745−752.
(65) Danckwerts, P. V. *Trans. Faraday Soc.* **1951**, *47*, 1014−1023.
(66) Kolb, C. E.; Worsnop, D. R.; Zahniser, M. S.; Davidovits, P.; Keyser, L. F.; Leu, M.-T.; Molina, M. J.; Hanson, D. R.; Ravishankara, A. R. Laboratory Studies of Atmospheric Heterogeneous Chemistry. In *Progress and Problems in Atmospheric Chemistry*; Barker, J. R., Ed.; World Scientific: Singapore, 1995; Vol. 3.
(67) Hanson, D. R. *J. Phys. Chem. B* **1997**, *101*, 4998−5001.
(68) Worsnop, D. R.; Morris, J. W.; Shi, Q.; Davidovits, P.; Kolb, C. E. *Geophys. Res. Lett.* **2002**, *29*, GL015542.
(69) Elliott, R. *Eutectic Solidification Processing: Crystalline and Glassy Alloys*; Butterworth & Co., Ltd.: London, 1983.
(70) Mullin, J. W. *Crystallization*, 4th ed.; Elsevier, Ltd.: Amsterdam, 2001.
(71) Mix 1. The composition of this multicomponent solution is as follows: OA = 40.11 wt %, LA = 2.33 wt %, MA = 6.14 wt %, palmitic acid = 33.98 wt %, stearic acid = 17.44 wt %.
(72) Mix 2. The composition of this multicomponent solution is as follows: OA = 38.11 wt %, LA = 7.11 wt %, palmitic acid = 32.16 wt %, stearic acid = 16.5 wt %, succinic acid = 0.84 wt %, glutaric acid = 0.76 wt %, adipic acid = 1.18 wt %, pentacosane = 8.08 wt %, hexadecanamide = 1.26 wt %.
(73) Mix 3. The composition of this multicomponent solution is as follows: OA = 33.86 wt %, LA = 1.97 wt %, MA = 5.15 wt %, palmitic acid = 28.69 wt %, stearic acid = 14.72 wt %, succinic acid = 0.714 wt %, glutaric acid = 0.62 wt %, adipic acid = 1.03 wt %, palmitoleic acid = 3.1 wt %, tetracosane = 1.23 wt %, pentacosane = 1.33 wt %, 2-pentadecanone = 1.38 wt %, 2-hexadecanone = 1.88 wt %, 2-octadecanone = 2.77 wt %, hexadecanamide = 1.57 wt %.
(74) Ostwald, W. *Z. Phys. Chem.* **1900**, *34*, 495−503.
(75) Lifshitz, I. M.; Slyozov, V. V. *J. Phys. Chem. Solids* **1961**, *19*, 31−50.
(76) Wagner, C. *Z. Elektrokhimiya* **1961**, *65*, 581−591.
(77) Ratke, L.; Voorhees, P. W. *Growth and Coarsening: Ostwald's Ripening in Materials Processing*; Springer: Berlin, 2002.
(78) Brooks, S. D.; Garland, R. M.; Wise, M. E.; Prenni, A. J.; Cushing, M.; Hewitt, E.; Tolbert, M. A. *J. Geophys. Res.* **2003**, *108*, 4487.
(79) Braban, C. F.; Abbatt, J. P. D. *Atmos. Chem. Phys.* **2004**, *4*, 1451−1459.
(80) Parsons, M. T.; Knopf, D. A.; Bertram, A. K. *J. Phys. Chem. A* **2004**, *108*, 11600−11608.
(81) Abelson, P. H. *Science* **1988**, *241*, 1569−1569.
(82) Meng, Z.; Dabdub, D.; Seinfeld, J. H. *Science* **1997**, *277*, 116−119.
(83) Seinfeld, J. H.; Pandis, S. N. *Atmospheric Chemistry and Physics*; John Wiley & Sons: New York, 1998.